Paper ID 10953 Session 2022
A2 / Power transformers & Reactors
PS1 / Experience and new requirements for transformers for renewable generation

On-line differential partial discharge measurements of condenser bushings on power transformers

Espen EBERG*
SINTEF Energy Research
Norway
Espen.eberg@sintef.no

Hans Kristian H MEYER
SINTEF Energy Research
Norway
kristian.meyer@sintef.no

Lars E. LUNDGAARD
SINTEF Energy Research
Norway
Lars.lundgaard@sintef.no

Asgeir MJELVE
Elvia
Norway
asgeir.mjelve@elvia.no

Stig KYRKJEEIDE
Mørenett AS
Norway
stig.kyrkjeeide@morenett.no

SUMMARY

Breakdown in condenser bushings on power transformers and reactors can have large consequences, such as transformer fire and long outage times. Failure statistics show that bushings are one of the most common failure causes/locations in transformers. To sustain security-of-supply and prolong transformer lifetime at an acceptable cost, targeted condition assessment of the bushing can be an effective agent.

Partial discharge (PD) measurements can provide valuable information about the health of the transformer bushing and can be sensitive to even very small defects. Applying on-line PD measurements on-site is challenging due to a noisy environment and uncertainty about the source of measured PD signals. Dielectric frequency response (DFR) is able to probe degradation by PD some time after PD initiation, but also other degradation mechanisms, such as moisture ingress, can give a similar DFR spectra. Dissolved gas analysis (DGA) can probe PD activity in the oil-insulated bushings, but for dry-insulated bushings, both old resin-bonded paper (RBP) and newer technologies such as resin-impregnated paper/synthetic (RIP/RIS) insulations, this is not an option.

On-line measurement using a full three-phase differential measurement scheme for PD have therefore been demonstrated on RBP and OIP bushings on-site. Measurement impedances were connected both directly to measurement taps, and differentially between measurement taps of all bushings. The results were compared to conventional PD measurements, both with frequency integration according to IEC 60270 and in the MHz range. With differential measurements it was possible to locate PD activity to one specific bushing, while common-mode noise was cancelled out. DGA of oil in the transformer main volume ruled out the winding as PD source. Being able to perform PD measurements on-site, using the presented three-phase differential PD measurement scheme, can thus be a valuable tool for detecting and localizing PD in three-phase high voltage components that are in service, where otherwise off-line assessment would require large power sources for excitation.

KEYWORDS

Partial discharge, PD , condenser bushing, condition assessment, dielectric frequency response, DFR, dissolved gas analysis, DGA

1 Introduction

Defects in condenser bushings cause a significant share of failures in power transformers, and the consequences are often catastrophic [1]. The risk of bushing failures can thus be the limiting factor for the lifetime prolongation of the transformer. Failures in bushings are often caused by insulation defects, oil leakage, moisture ingress, and are accelerated by electric and/or thermal stresses. To prevent bushing failures, there is a need for cost-efficient and accurate methods for bushing condition assessment.

The insulation system of condenser type bushings consists of both an inner insulation (condenser core) and an external insulation with a ceramic or polymer housing. The condenser core distributes the field by coaxial conductive layers of aluminium foil separated by insulating paper or synthetic foils which is either impregnated with oil or resin. The insulation technologies used are called OIP (oil impregnated paper), RBP (resin bonded paper), RIP (resin impregnated paper) and RIS (resin impregnated synthetics). The outer aluminium foil is connected to a test tap on the flange and provides a capacitive probe that can be used for diagnostic measurements of the insulation system in both bushing and transformer. Some parameters, such as bushing capacitance, dissipation factor and partial discharges can be monitored on-line at power frequency using the test tap. As the test tap is a sensitive item in the bushing design and connected to ground in normal operation, the risks involved with on-line monitoring must be carefully considered [2].

Dielectric frequency response (DFR) and dissolved gas analysis (DGA) are state-of-the-art techniques for condition assessment of high voltage bushings and transformers on-site. In DFR measurements the complex permittivity is measured over a broad frequency range, 1 mHz to 1 kHz normally. The technique is sensitive to common failure modes in bushings, such as moisture ingress, short-circuited foils and degradation caused by PD [1]. The combination of DFR and DGA have proven to be sensitive to degradation of OIP bushings [3]. However, DFR is not applicable on-line, and DGA may lose relevance for bushing condition assessment as the industry is moving toward dry-type bushings. Moreover, performing DGA on bushings involves a risk as the oil volume is exposed during sampling of the oil.

Measurement of partial discharges (PDs) can be an accurate diagnosis method for transformers and bushings [4] and is part of the factory acceptance test (FAT) and site acceptance test (SAT), but rarely applied on-site for assessment of bushings. PD measurements can detect developing insulation faults at a very early stage and could especially be useful to complement DFR measurements where DGA is not applicable, for instance on dry-type bushings, and PD from voids/cracks within the condenser body can become a more prominent failure mechanism. As a tool for condition assessment, PD measurements are best suited in a shielded laboratory environment. On-site, PD measurements suffer from external noise and signal crosstalk between phases. Electromagnetic interference in the field can be reduced by adjusting the PD integration frequency and by using galvanically isolated PD coupling devices such as high- frequency transformers or antennas [5]. Antennas may also be used to gate out external noise in the measurements.

It is advantageous to not only detect PD, but also to locate the PD source. For on-line measurements, it can be difficult to pin-point the partial discharge origin, as there are many candidate sources in a substation. The sources can to some extent be localized by comparing the PD signals with injected calibration signals in both the time and frequency domain [6] or by signal amplitude correlation [7]–[9]. The path-dependent damping and shaping of a PD signal from its origin to the measurement terminal is the basis for these methods. Acoustical methods are also routinely used to localize PD in power transformers [6], [8]–[10].

Another approach to reduce external interference and to localize PD is to use differential PD measurements, similar to a bridge measurement. In this paper, we show that differential methods for three-phase PD measurements applied on a transformer in service in the field can handle noise and be used to locate discharges to specific phases. The technique was tested in a laboratory setup, and in field

measurements on both 132 kV OIP and RBP transformer bushings. DFR and DGA measurements were also performed or available to evaluate the agreement of the different condition assessment techniques.

2 Method

2.1 On-line differential three phase measurements

The proposed differential measurement setup is shown in Figure 1 for a power transformer with bushings equipped with test taps. There are six PD quadrupoles that are connected to the bushing test taps. Three quadrupoles (Z_A, Z_B and Z_C) are connected between the test tap and ground in the conventional way, while three quadrupoles (Z_{A-C}, Z_{A-B} and Z_{B-C}) are connected differentially between test taps. The connection scheme shown in Figure 1 (a) allows for separation of different PD sources per phase, by detecting where the various PD signatures appear. In Figure 1 (b) and (c) images show how the connections were made in practice on a transformer. The differentially connected quadrupoles were isolated from the transformer tank. The neutral point bushing has not been included in the PD measurement scheme.

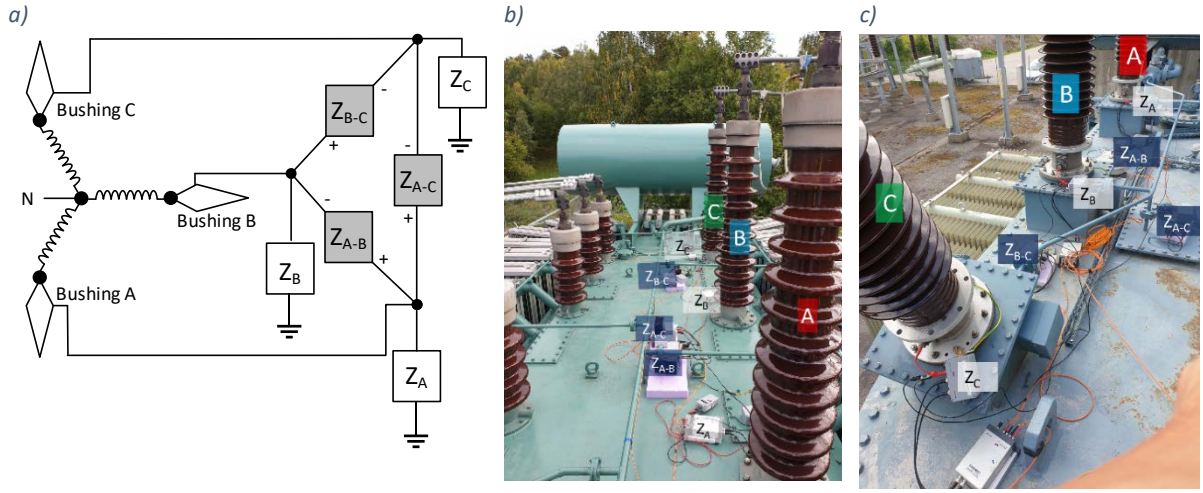

Figure 1: a) Three-phase differential measurement setup on power transformer bushings. Quadrupoles Z_A, Z_B and Z_C are connected between each bushing test tap and ground, while Z_{A-C}, Z_{A-B} and Z_{B-C} are connected differentially between the taps. The polarities of the terminals on the differential units are also indicated in the figure. b) measurement on RBP bushings, and c) measurement on OIP bushings.

Common mode signals and noise that occur equally on all phases are suppressed in the differential quadrupoles, while signals from PD sources in one phase, e.g. PD from within the bushing, will be suppressed in only one of the differential quadrupoles. PD signals from inside the transformer, such as from the windings, will also be present in the measurements, but internal PD in the transformer is detectable in routine dissolved gas analysis (DGA) of the transformer oil and should be part of the asset management of the transformer fleet.

Table 1 shows the expected signal occurrence in the different quadrupoles in Figure 1 from various PD sources in the ideal case, and have been verified by circuit simulations and laboratory tests reported in [11]. Three different cases can be expected:

1) **Signal occurrence between a single phase and ground:** e.g. a source in phase A will normally occur in all quadrupoles except Z_{B-C}, which is the quadrupole between the measurement taps of the bushings on phase B and phase C. The signal will be strongest in phase A, and lower in phases B and C.
2) **Signal occurrence between two phases:** Phase-to-phase discharges will be suppressed in an equally characteristic manner in the network. For example, discharges between phase A and B will normally occur in all quadrupoles except Z_C. Furthermore, they will be stronger in Z_{A-B} than in Z_{B-C} and Z_{A-C}.
3) **External noise or PD:** External noise, which is equally radiated into all phases will, on the other hand, be suppressed in all three differential quadrupoles Z_{A-C}, Z_{A-B} and Z_{B-C}.

Table 1: Signal Matrix. Uppercase X (green) marks strong signal occurrence, lowercase x (yellow) marks signal occurrence and – (red) marks signal suppression, based on simplified circuit simulations

PD source	Signal in quadrupole					
	Z_A	Z_B	Z_C	Z_{A-C}	Z_{A-B}	Z_{B-C}
Phase A	X	x	x	X	X	-
Phase B	x	X	x	-	X	X
Phase C	x	x	X	X	-	X
Between A and C	X	-	X	X	x	x
Between A and B	X	X	-	x	X	x
Between B and C	-	X	X	x	x	X
External noise	X	X	X	-	-	-

The measurement impedances and acquisition units used in this work were Omicron CPL 542 and MPD 600 respectively. We found that broadband IEC 60270 compatible integration frequencies did not give an acceptable signal-to-noise ratio (SNR) in all cases. Hence, an optimal frequency integration band was found using the software FFT for the measurement system.

According to IEC 60270, PD measurements are calibrated by injecting pulses of known charge magnitude into the terminals of the unenergized test object. In the case of the differential measuring scheme, the voltage will distribute in the impedance network and a direct interpretation of calibrated apparent charge is challenging. To acquire the expected cancellation in the differential units it is still important that they are adjusted to a known pulse size so that the interpretation scheme in Table 1 can be applied. The calibration scheme followed, was to connect quadrupoles between test tap and ground and perform calibration according to IEC 60270. The "calibration procedure" was also repeated at several frequency bands above 1 MHz, so PD levels could be adjusted in post-processing for measurement executed in other frequency bands. The variation in calibration factor was 5 % between units, and the calibration of differential units was set to the average value of calibration factor for the chosen frequency band.

2.2 Dielectric frequency response

DFR measurements were performed with the transformer disconnected from the grid. The low voltage (LV) side bushings were connected to ground. The bushings on the high voltage (HV) side were connected in parallel and connected to the voltage source of the DFR instrument (IDAX 300), and the test tap was grounded on the bushings not measured. A frequency spectrum of 1 mHz to 1 kHz was used, except for the N phase on the OIP bushing where 2 mHz was minimum frequency.

2.3 Field measurements of partial discharges

On-site measurements were carried out on two transformers in service. The objective of the measurements was to verify and refine the differential measurement setup.

2.3.1 Transformer with RBP bushings

A 132/49 kV, 130 MVA (YNyn0) power transformer from 1978 with resin-bonded paper (RBP) bushings was made available for measurements. In the routine tests for RBP bushings according to the standard IEC 60137, up to 100 pC at 105 % of the maximum phase-to-earth operating voltage is tolerated. For demonstrating the differential technique, RBP bushings are therefore useful as test objects. Annual, routine oil testing and DGA of the transformer oil have not indicated internal PD in this transformer.

The transformer was first energized from the low-voltage side, with the 132 kV line disconnected to reduce line fed noise. As there was no field shielding available on the bushings, corona discharges from the bushing top appeared during these tests. The tests were also repeated with the 132 kV line connected and energized, which eliminated the corona discharge activity. Both these tests were reported previously in [11]. One year later, tests were made with corona rings mounted on the bushings. In addition to the differential measurements, calibrated PD measurements according to IEC 60270 were made without differential impedances. None of the tests produced discharge levels above 100 pC while the 132 kV line was connected.

2.3.2 Transformer with OIP bushings

The second test object was a 132/22 kV, 31.5 MVA (YNyn0) power transformer from 1986 with OIP bushings. The bushings were scheduled for replacement due to oil leakage. The oil level was topped up on bushing B and C and put into service while awaiting replacement.

The transformer was connected to the grid from both 22 kV and 132 kV sides during measurement. Conventional PD measurements according to IEC 60270 and at higher integration frequencies were conducted prior to differential measurements.

3 Results and discussion

3.1 Resin-bonded-paper bushings

3.1.1 Dielectric frequency response

In Figure 2 DFR measurements for the condenser body C_1 are shown, with tan(δ) in (a) and capacitance in (b), respectively. There was no history of DFR measurements for these bushings, but nameplate C_1 values at 50 Hz corresponded well to the measured values and tan(δ) were within requirements in IEC 60137 [12]. For low frequencies tan(δ) collapses to negative values for all phases, and these datapoints are not shown. Negative values for tan(δ) occur when conductive paths along surfaces, inside or outside the bushing, short circuit the higher resistive path through the condenser body [13]. Since also the N phase shows the same behaviour at low frequencies it is unlikely that deposits from e.g. surface PD within the bushing is the cause. Deposits on the outer surface is ruled out by proper cleaning prior to measurement. It is thus likely that creepage currents arise from high conductivity of the oil within the bushing housing or along the lower part of the condenser body interfacing the transformer oil. As this is a dry-type bushing the consequences of degraded condition of the interfacing oil is less severe than for OIP bushings.

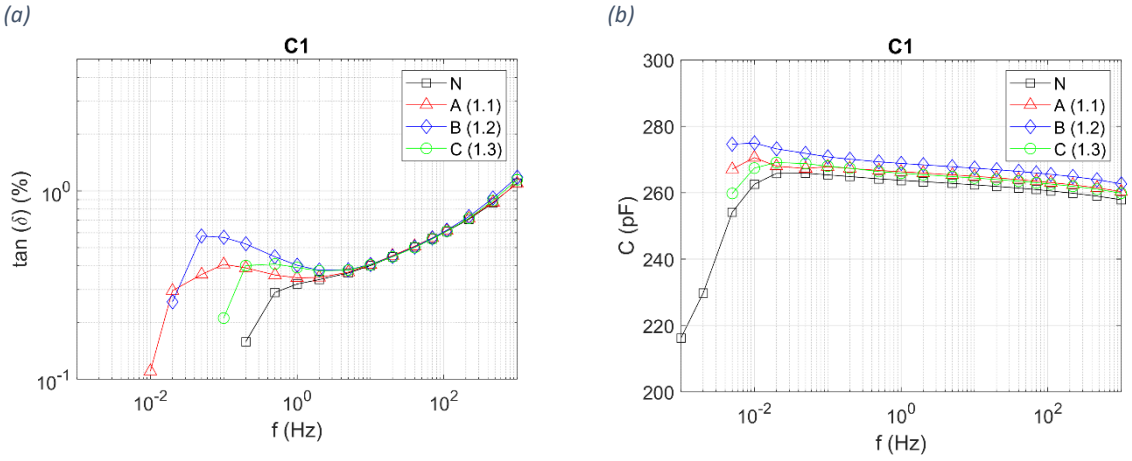

Figure 2: (a) tan(δ) and (b) capacitance of condenser body (C_1) in the 132 kV RBP bushing.

3.1.2 Three-phase differential partial discharge measurements on RBP bushings

The 132 kV line was disconnected, and field grading rings were mounted on the transformer bushings to suppress the corona discharges. A different PD integration frequency band (450-550 kHz instead of 75-725 kHz as in [11]) was used, as the noise level in the station had increased. Some results from the field tests are shown in phase-resolved partial discharge (PRPD) plots in Figure 3. The upper row of PRPD plots were recorded with quadrupoles between the bushing measurement taps and ground (Z_A , Z_B and Z_C), while the lower row shows the differential quadrupoles Z_{A-C} , Z_{A-B} and Z_{B-C}. Note the more severe noise interference in the upper row compared to the lower row. The experience is that noise in this range varies from day-to-day, but the differential method provides efficient supression.

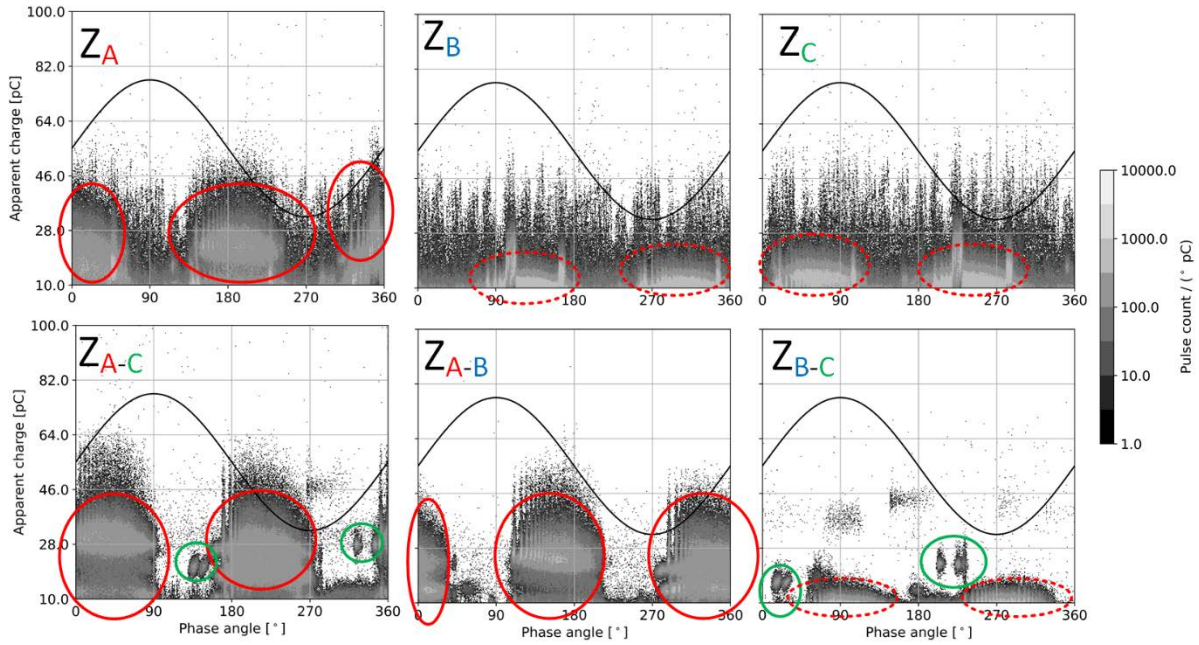

Figure 3: PRPDA results from field test on RBP bushings measurements, with internal discharges in phase A and C. The PD integration frequency was 450 to 550 kHz. Discharge phase localization is indicated with red (discharges in phase A) and green (discharges from phase C) circles. For the conventional impedances Z_A, Z_B and Z_C, the broken line circles indicate discharges from another phase.

Discharge clusters highlighted with red circles in Figure 3 originate from phase A, according to Table 1. When studying the upper row PRPDs, it appears that the red highlighted discharge clusters in phase A occur partly on the rising flanks and occur a bit before the voltage zero-crossing. This could indicate a form of void discharge. Another possibility is that the discharges originate from a floating conductive element or a poor connection. Similar findings were reported in the earlier field test [11], and there seems to be no changes in PD activity in the bushings.

Other discharge clusters highlighted with green circles are missing in the lower middle plot (Z_{A-B}). These discharges should therefore originate in phase C. Due to noise, or the large discharges originating in phase A, the discharges originating from phase C are not clearly visible in the upper right plot. The discharge patterns are somewhat different, especially the discharges in phase C, which were distributed over a larger phase angle in previsous measurements [11]. The observed differences could be related to physical changes in the PD phenomena, or to measurement factors such as PD integration frequency bands and different levels of noise interference.

3.2 Oil-in-paper bushings

3.2.1 Dielectric frequency response

In Figure 4, DFR measurements for the condenser body C_1 are shown, with tan(δ) in (a) and capacitance in (b), respectively. Phase C and N have monotonically increasing tan(δ) for reduced frequencies, and levels of tan(δ) at low frequencies are comparable to service aged bushing of similar age and insulation system. They are significantly lower than severely degraded OIP bushing with PD-activity that have been tested in the laboratory.

For phase B, the same collapse in tan(δ) at low frequencies is seen as for the RBP bushings, which could indicate creepage currents [13]. A small ridge in the tan(δ) curve for low frequencies can also be seen for phase A. In the measurement of C_1 capacitance, phase A and B also differs from C and N, with a small decrease at the lowest frequency. This behaviour is also similar to what was seen for the RBP bushings, but less pronounced. Since the DFR spectra differs between the phases, it is likely that the origin to the diverging spectra in phase B, and likely A, is related to the bushing.

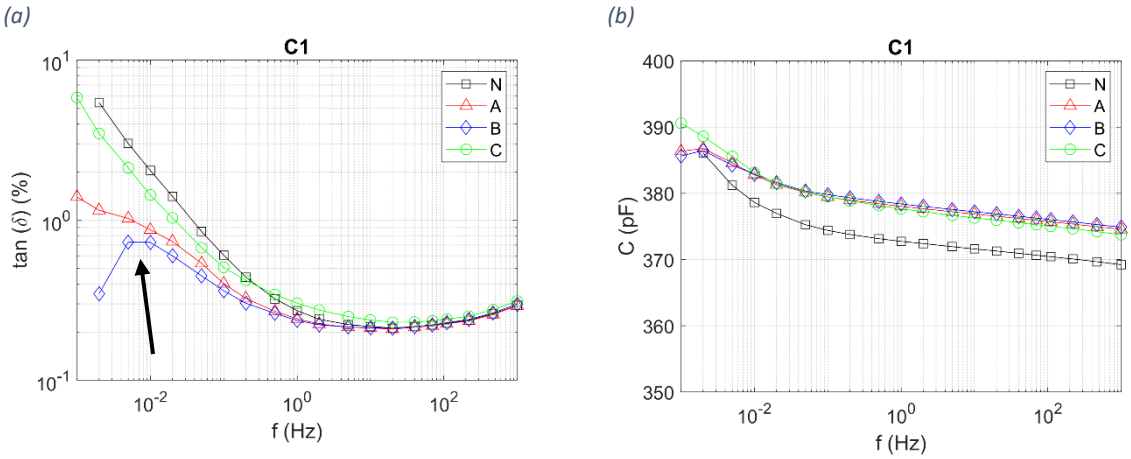

Figure 4: (a) tan(δ) and (b) capacitance of condenser body C1 in the 132 kV OIP bushings. The DFR measurement on phase N was stopped at 2 mHz due to time constraints and forecasted rain.

3.2.2 Three-phase differential partial discharge measurements on OIP bushings

In Figure 5 and Figure 6, the PRPD patterns for PD measurements without the three-phase differential setup are shown for integration frequency bands 75-725 kHz (in compliance with IEC 60270) and 1.5 MHz to 2.5 MHz respectively. For the IEC-compliant measurements in Figure 5 there are high levels of noise, making it impossible to interpret the PRPD-patterns in any way. By increasing the frequency of the integration band to the MHz-range, most of the irradiated and conducted external noise is damped, as seen in Figure 6. For each phase there are now clusters of PD that can visually be separated.

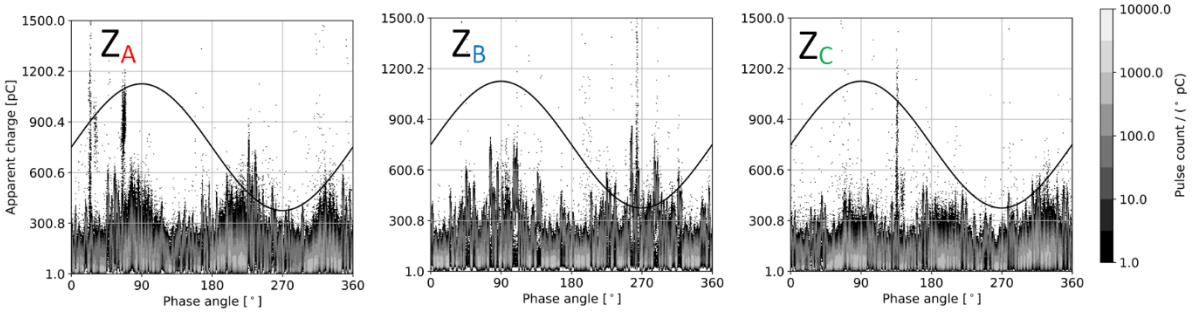

Figure 5: PRPD patterns for conventional three phase measurements (i.e., without differential measurement network) with integration bandwidth 75-725 kHz, in compliance with IEC 60270.

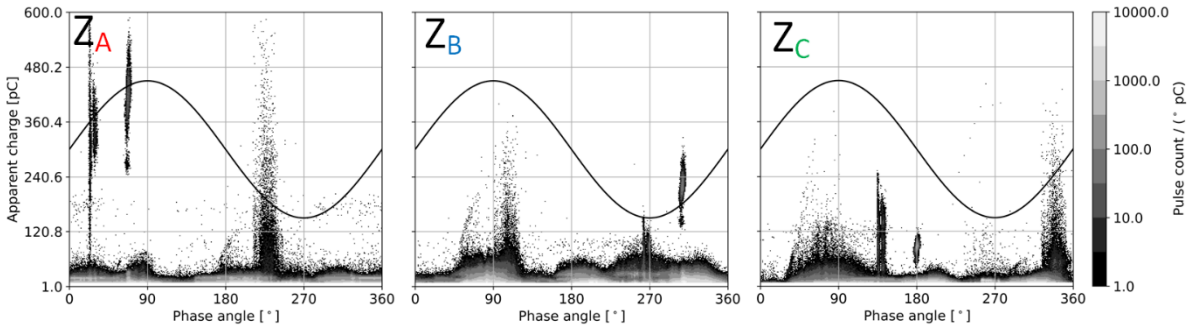

Figure 6 PRPD patterns for conventional three phase measurements (i.e., without differential measurement network) with non-conventional integration band (1.5 MHz to 2.5 MHz).

In Figure 7 the PRPD plots using the differential measurement scheme is shown. Due to grid noise, it was necessary to use a non-conventional PD integration band (1.65 to 1.95 MHz) for these measurements. It was considered crucial to use a low, but non-noisy frequency band, since the high-frequency performance of the measurement network is likely poor.

It was observed that the greatest PD-activity for the impedances connected between test tap and ground was seen in Z_B (marked with a blue circle). Likewise, for the differential measuring impedances the bulk of PD-activity is found for Z_{A-B} and Z_{B-C}. According to the interpretation diagram in Table 1, this allocates much of the recorded PD-activity to phase B. Combined with the DFR-spectrum for phase B in Figure 4, indicating creepage currents within the bushing, it is concluded that the PD has been initiated within this bushing.

Furthermore, a narrow, but relatively high-amplitude discharge cluster was observed at the peak of the line voltage between phase A and B (highlighted with purple circles in Figure 7). This discharge cluster is, with basis in Table 1, interpreted as interphase discharges between phase A and B. The interpretation is supported by the fact that the discharges are most suppressed in Z_C, that they are stronger in Z_{A-B} than in the two other differential units, and that the discharges occur when the Z_{A-B} line voltage is at its peak. Interphase discharges in a transformer seems unlikely, so this defect may well come from external or auxiliary equipment, e.g. a single-phase load or tap changer leads.

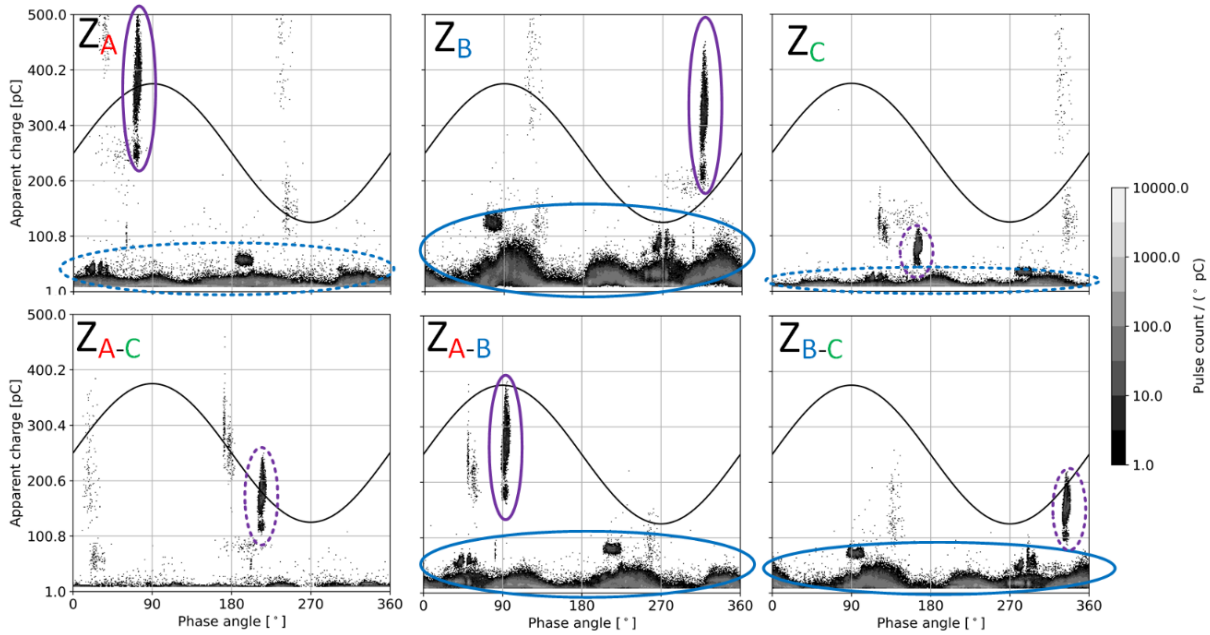

Figure 7: PRPDA results from field test on OIP bushings 132 kV line connected with discharges from phase B (blue circles) and discharges between phase A and phase B (purple circles). Note that the discharges between phase A and B occur when the voltage between phase A and B is at its peak (at 90° in Z_{A-B}). The broken line circles indicate cross-coupled discharge signals according to Table 1. The PD integration frequency was 1.65 to 1.95 MHz, as the IEC 60270 band (< 1 MHz) suffered from noise.

Coupling devices in a differential measurement setup should preferably have tuneable input impedances to optimize the common mode rejection ratio. In the setup used here, however, all the coupling impedances had 50 Ω inputs. Due to the impedance network arrangement, the equivalent input impedance for incoming PD pulses at any of the three measurement taps is 25 Ω. Moreover, the high-frequency performance of the measurement network is poor as the signal path is a distributed network of wires of around 50 cm lengths each and not impedance-matched coaxial cables.

4 Conclusions

A three-phase differential PD measurement system has been tested on-site on two transformers with RBP and OIP bushings, respectively, after proof-of-concept tests in the lab. The system worked as expected and enabled localization of PD sources from the different transformer phases

In case of the OIP bushing, the differential measurements scheme was able to allocate PD activity to a specific phase and in coherence with the DFR-measurements. This demonstrates that the differential PD-measurements can provide more decisive information about the condition of the bushings, as DFR alone in this case would indicate PD as only one of the defect types that gives creepage currents. DGA would be able to give decisive information.

With the shift to new dry-type bushings (RIS) it is expected that PD-measurement will become an even more relevant condition assessment method, since DFR is likely to be less sensitive to internal failures such as voids and cracks, especially in an early phase.

The method has the advantage of allowing in-the-field measurement on a transformer energized from the grid, thus avoiding use of special test transformers for energizing. The method could also be a useful tool for PD localization in multi- phase HV equipment in general. Future work should concentrate on improving the high frequency (> 5 MHz) properties by applying coupling units/sensors with passband in this range and proper impedance matching.

ACKNOWLEDGEMENTS

This work has been funded by the Norwegian Water Resources and Energy Directorate (NVE), Agder Energi Nett, Arva, Elvia, Tensio TS, BKK Produksjon, Fagne, Hydro Energy, Mørenett, Statkraft, Statnett and Hitachi Energy through the joint industry project "Condition Assessment of Transformer Bushings".

BIBLIOGRAPHY

[1] Working Group A2.43 CIGRE. "Transformer bushing reliability" (Technical Brochure 755, February 2019)

[2] L. Jonsson. "Advantages vs. risks with on-line monitoring of transformer bushings" (IEEE Electrical Insulation Conference, June 2021, pages 556–559)

[3] L. Jonsson, L. Melzer, N. Schönborg, and G.-O. Persson. "Experimental evaluation of status of 400 kV shunt reactor bushings in the Swedish national grid" (CIGRE Session Paris, August 2018, pages A2-203)

[4] W. Koltunowicz and L.-V. Badicu. "Challenges in Monitoring of Power Transformers" (My Transfo 2016, November 2016)

[5] Working Group D1.37 CIGRE. "Guidelines for partial discharge detection using conventional (IEC 60270) and unconventional methods" (Techincal Brochure 662, August 2016)

[6] J. Fuhr and T. Aschwanden. "Identification and localization of PD-sources in power-transformers and power-generators" (IEEE Transactions on Dielectrics and Electrical Insulation, February 2017, vol. 24, no. 1, pages 17–30)

[7] K. Rethmeier, M. Kruger, A. Kraetge, R. Plath, W. Koltunowicz, A. Obralic, and W. Kalkner. "Experiences in on-site partial discharge measurements and prospects for PD monitoring" (2008 International Conference on Condition Monitoring and Diagnosis, April 2008, pages 1279–1283)

[8] U. Ranninger and M. Krüger. "Measurement, localisation, and monitoring of partial discharges on a power transformer" (Transformers Magazine, January 2021, vol.8, no 1)

[9] M. Krüger, U. Ranninger, and L. V. Badicu. "Monitoring, diagnosis and fault finding on a power transformer" (Transformers Magazine, July 2015, vol. 2, no. 3, pages 30–37)

[10] L. E. Lundgaard. "Partial discharge. XIV. Acoustic partial discharge detection-practical application" (IEEE Electrical Insulation Magazine, September 1992, vol. 8, no. 5, pages 34–43)

[11] H. K. H. Meyer, E. Eberg, and L. Lundgaard. "On-line three-phase differential partial discharge localization in transformer bushings" (IEEE Electrical Insulation Conference, June 2021, pages 80-83)

[12] International Electrotechnical Commission. "IEC 60137:2017 - Insulated bushings for alternating voltages above 1000 V" (2017)

[13] F. Huellmandel, M. Appold, A. Kuechler, R. Krump, and J. Titze. "Condition assesment of high voltage bushings by means of dielectric diagnosis with pdc" (15th International Symposium on High Voltage Engineering, 2007, T7-172, pages 1-6)